Electronic Supplementary Material (ESI) for Nanoscale Horizons.

Supporting Information: Plasmon-Enhanced Photoresponse of a Single Silver Nanowire and its Networked Devices

Mohammadali Razeghi[1], Merve Üstünçelik[1], Farzan Shabani[1], Hilmi Volkan Demir[1,2,3,4], T. Serkan Kasırga[1,2*]

[1] Institute of Materials Science and Nanotechnology – UNAM, Bilkent University, Ankara 06800, Turkey

[2] Department of Physics, Bilkent University, Ankara 06800, Turkey

[3] Department of Electrical and Electronics Engineering, Bilkent University, Ankara 06800, Turkey

[4] LUMINOUS! Centre of Excellence for Semiconductor Lighting and Displays, The Photonics Institute, School of Electrical and Electronic Engineering, School of Physical and Mathematical Sciences, School of Materials Science and Engineering Nanyang Technological University, Singapore 639798, Singapore

*Corresponding author email: kasirga@unam.bilkent.edu.tr

Scanning Photocurrent Microscopy Experimental Setup

The scanning photocurrent microscope (SPCM) used in the experiments is a commercially available setup from LST Scientific Inst. Ltd. The setup consists of a scanning microscope that simultaneously provides a wide field view and the reflected light intensity. The laser beam is focused with an Olympus 40x 0.6NA ULWD objective with compensation collar. This creates a ~400 nm resolution for 532 nm excitation wavelength, determined by Gaussian fitting the first derivative of the intensity profile across an ultra-steep metal contact edge. The scanner can take 25 nm steps and scan size can be selected from 100 nm to 2.5 cm. The laser power incident on the sample is continuously monitored and registered by a calibrated power meter. The incident laser power can be tuned with a variable neutral density filter. The laser beam is chopped at 2 kHz via a mechanical chopper for phase sensitive detection of the photocurrent via a lock-in amplifier. The generated current is amplified with an SR570 current pre-amplifier, and the output of the amplified signal is fed to SR 830 lock-in amplifier. This allows very high sensitivity of the detected photo-response down to a few picoamperes. The bias is applied through the SR570 or an external voltage source.

The polarization dependent studies are performed using 632.8 nm HeNe laser source unless otherwise stated. We also performed similar measurements with 532 nm laser. The laser beam produced by both HeNe and 532 nm source are linearly polarized. To obtain a high extinction ratio, we aligned a linear polarizer with the polarization of the laser source. To rotate the polarization angle with respect to the sample, we used a quarter wave plate (QWP) with a linear polarizer (LP) on a rotational mount as the analyzer. **Figure S1a** shows the schematic of the polarization control configuration in the SPCM setup. **Figure S1b** shows laser power vs. analyzer angle. The intensity variation is less than 1% except 330°. The polarization angle dependent photocurrent and photoconductance data reported in the main text is read from the SPCM photocurrent maps. This eliminates the possible laser beam shift caused signal changes.

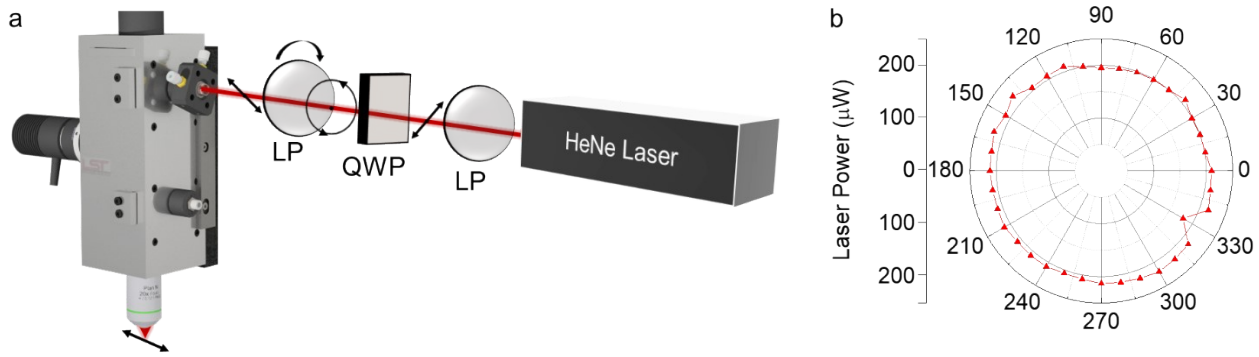

Figure S1 a. SPCM configuration with the polarization control optics. **b.** Laser power vs. analyzer angle shows that the laser power change for different angles is very small.

Characterization of Silver Nanowires

For the experiments reported in this paper, we used commercial Ag NWs from Sigma-Aldrich (Product code: 778095). Nanowires are 120-150 nm in diameter and 20-50 μm in length and provided as 0.5% isopropyl alcohol (IPA) suspension.

We used Raman spectroscopy, XRD and XPS to characterize the nanowires. **Figure S1a** shows the Raman spectrum taken from a dense region of nanowires. Ag NWs exhibit a featureless Raman spectrum, however, the polyvinylpyrrolidone (PVP) coverage over the nanowires due to the inherent residue of the polyol process shows three pronounced peaks at 237, 1337 and 1605 cm^{-1}. We also observed a broad peak around 2900 cm^{-1}. These peaks agree with those reported in the literature. **Figure S1b** shows the XRD θ-2θ scan of the silver nanowires deposited on glass substrate. Finally, XPS survey given in **Figure S1c** shows that the full width at half maximum for the Lorentzian fits to the Ag $3d_{5/2}$ and Ag $3d_{3/2}$ peaks are ~0.6 eV and no other Lorentzian can be fitted under the peaks. Thus, we infer that the freshly deposited nanowires are in pure metal form.

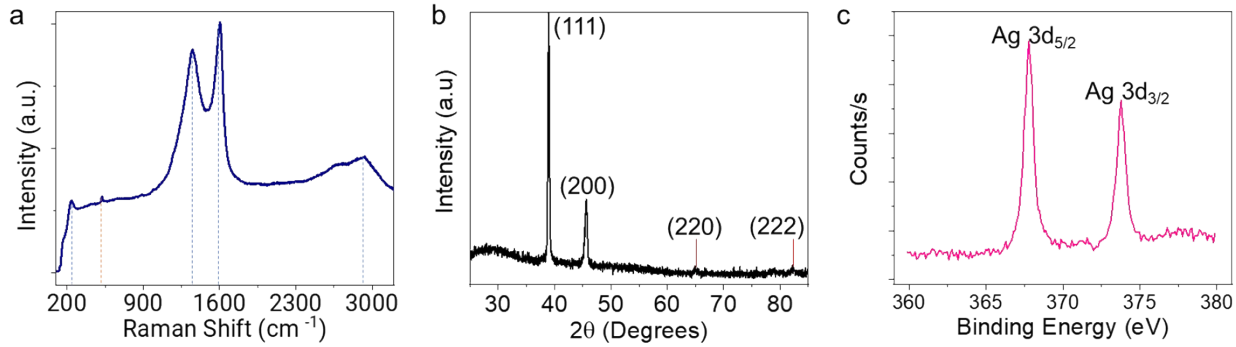

Figure S2 a. Raman spectrum taken from an Ag NW. Blue dashed lines indicate the PVP spectra and the orange dashed line shows the Raman mode of the substrate. **b.** XRD scan shows all the major diffraction peaks of Ag NWs. **c.** XPS spectrum of Ag 3d peaks. The peaks can be fitted with single Lorentzian function, showing that there are no oxidation states for freshly prepared devices.

Finite Element Method Simulations of Resistance Change in Silver Nanowires

We performed finite element method (FEM) simulations to obtain an estimate on how much temperature rise is required to reach the experimentally measured resistance change in the

devices. We used COMSOL Multiphysics simulation package to perform these simulations. Two 20 μm long cylindrical nanowires with 150 nm diameter was modelled over a glass slate. The ends of the nanowires were fixed at the ambient temperature. A thermal contact was defined across the glass substrate and the Ag NW. To model the SPP assisted local heating, we defined a point heat source with a 100 nm radius at the junction of the NWs. **Figure S3a** shows the temperature distribution over the nanowire. **Figure S3b** shows the resistance change (δR) and the maximum temperature rise (δT_{max}) under varied heat input.

We also would like to provide a theoretical analysis for the bolometric response of the device shown in **Figure 3e**. For a small temperature rise $\delta T(x)$, where coordinate x runs from 0 to 1 from right to left contact, the conductance change can be estimated as $G_{Ph} \approx -\frac{1}{R^2}\frac{dR}{dT}\delta T_l$. Here δT_l is the temperature change under the laser spot and $R(T)$ is the resistance of the nanowire. With this formula, we can estimate the order of magnitude of G_{Ph} for the device reported in Figure 3e. If we take the resistance as ~160 Ω and $\frac{dR}{dT} \approx 0.4\ \Omega/K$ based on the Resistance vs. temperature graph and $\delta T_l \approx 0.5\ K$ from the Comsol simulations, we obtain $G_{Ph} \approx$ -0.7 μS which is slightly larger than our measurements. Here, δT_l value might be overestimated as the Comsol simulation assumed the heating at the junction of two nanowires.

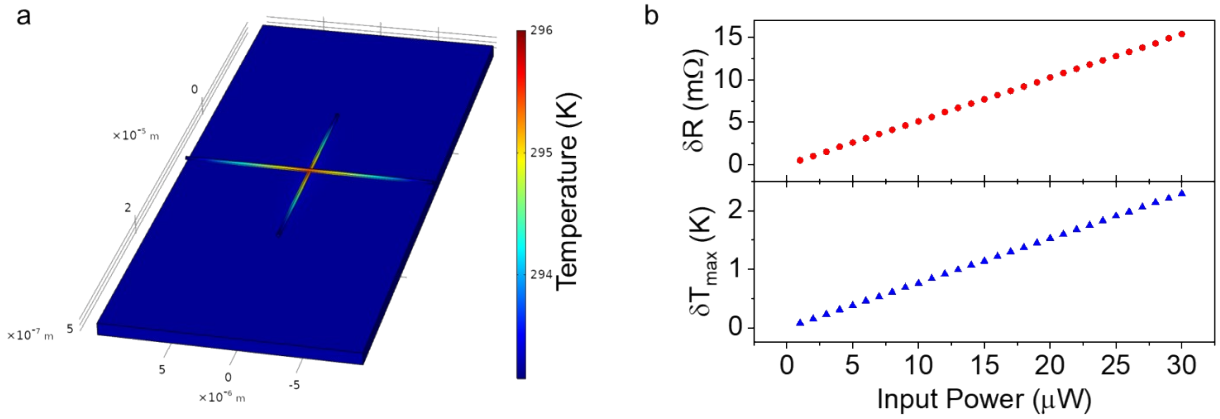

Figure S3 a. Thermal surface map of the NW modelled on a glass substrate under 30 μW heat input. **b.** The graph shows the resistance change δR in the upper panel and the maximum temperature on the NW, δT_{max}, in the lower panel. δR and δT_{max} values agree with the experimentally determined values reported in the main text.

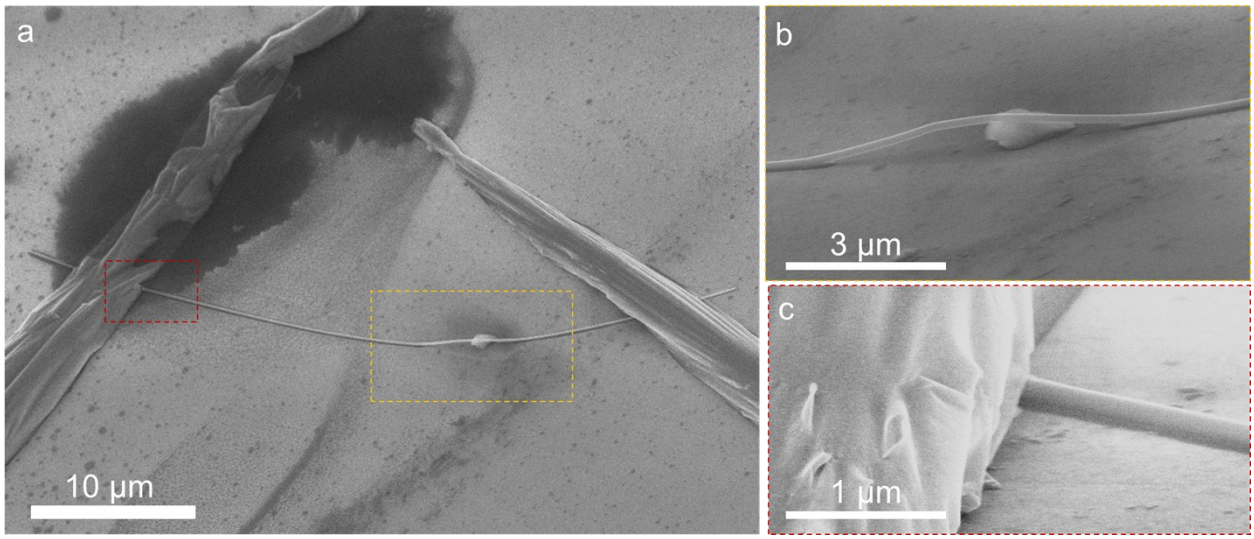

Figure S4 a. SEM image of the device measured in Figure 3e in the main text. Colored regions correspond to zoomed in sections shown in **b** and **c. b.** Bulged section of the nanowire is shown. The photoresponse is enhanced in the vicinity of the bulged region. **c.** Close-up image of the NW-indium junction.

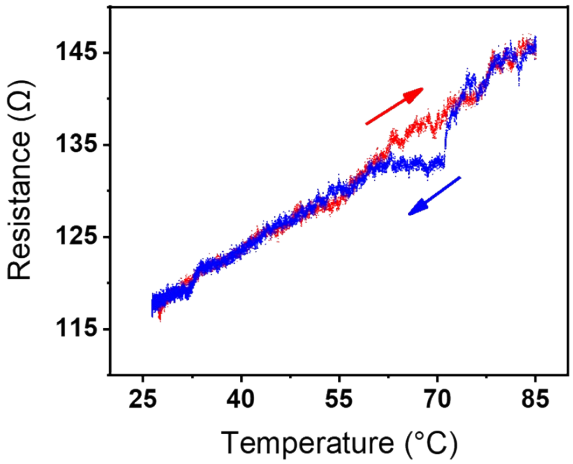

Figure S5 Resistance vs. temperature graph of a Ag NW network device shows the bolometric response of two-terminal resistance upon heating(red) and cooling (blue).

Comments on the origin of the alternating zero-bias signal on single Ag NW device

Zero-bias response reported in Figure 3h-II shows successively alternating I_{min} and I_{max} points. Close-up SEM images of the NW shows that the nanowire has split into two segments that are very close to each other as shown in **Figure S6**. When comparing the section between the contacts to the section beyond the contacts, it can be seen that some mass has been transported between the two segments and left some undulations leading to a distinguished response. A similar response is observed due to the mass transport in a different device shown in **Figure S7**. The SPCM maps show a bipolar response at an arbitrary point of the Ag NW. After several

measurements, the wire broke from the point where the photoresponse is observed. This is an interesting phenomenon that requires further investigation.

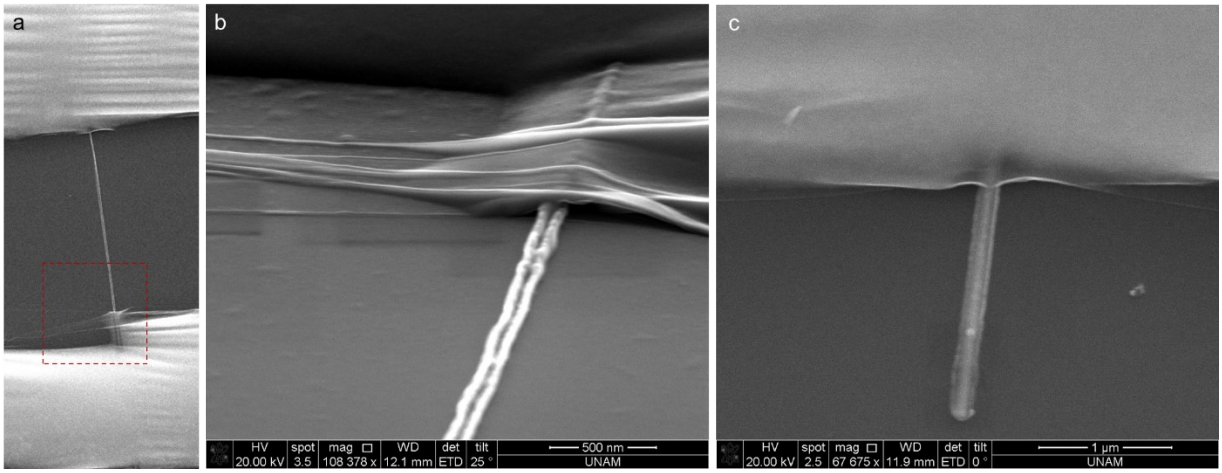

Figure S6 a. Mirrored SEM image of the device given in the main text. **b.** Close up view of the indium-Ag NW region after many measurements under bias. **c.** Tail of the Ag NW beyond the indium.

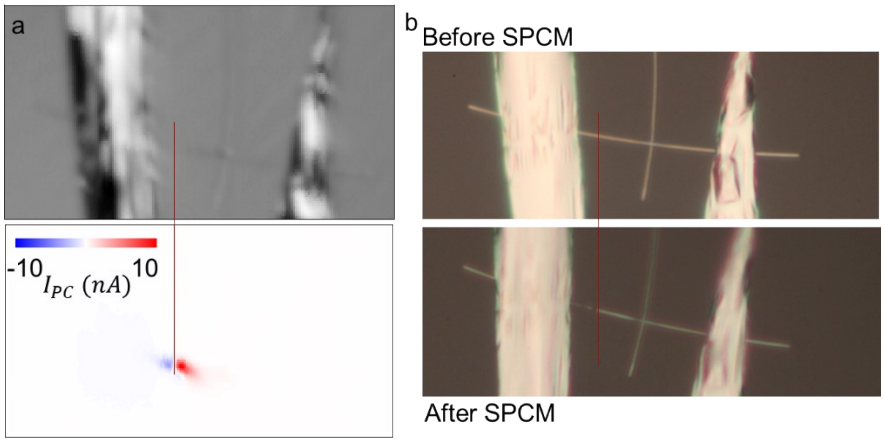

Figure S7 a. SPCM measurements on a single wire device. Red line is drawn to guide the eye for the spatial position of the photoresponse. **b.** Before and after optical microscope images of the device. Location of the photoresponse is marked with the red line on both images.

Synthesis of silver nanoparticles (Ag NPs)

Ag NPs were synthesized according to a published recipe in the literature[1] (Ref. 40 in the Main Text), with some modifications. Silver nitrate ($AgNO_3$, ≥99.0%), 1-octadecene (ODE, 90%), oleylamine (OLA, 70%), ethanol (absolute), toluene (≥99.5%) and n-hexane (≥97.0%) from Sigma Aldrich are used in the synthesis process. In a typical synthesis, 30 mL of ODE, 15 mL of OLA and 600 mg of $AgNO_3$ were mixed in a 100 mL three-neck flask. The solution was kept under vacuum for 2 h at room temperature to remove the oxygen and other volatile species. Then, the flask was flushed with argon gas and the temperature was raised to 180 ˚C with heating rate of 7 ˚C/min. As the temperature was increasing, the color of the solution turned into light orange, green

and finally black, which is an indicative of Ag NPs formation. The flask stayed at this temperature to have a complete nucleation and growth process, and then the temperature was decreased to 150 ˚C to focus the size of the Ag NPs through Ostwald ripening. After an extra 2 h, the heating mantle was removed, and the solution was diluted with hexane at room temperature. The collected solution was centrifuged at 5000 rpm for 6 min to remove the unstable or large NPs. Ag NPs were separated from the solution and unwanted species by addition of extra ethanol and centrifugation at 5000 rpm for 10 min. Finally, the precipitate was redispersed in toluene and kept in refrigerator for further use.

(1) Chen, M.; Feng, Y. G.; Wang, X.; Li, T. C.; Zhang, J. Y.; Qian, D. J. Silver Nanoparticles Capped by Oleylamine: Formation, Growth, and Self-Organization. *Langmuir* **2007**, *23* (10), 5296–5304. https://doi.org/10.1021/la700553d.